Influence of crosslinker amount on the microstructure and properties of starch-based superabsorbent polymers by one-step preparation at high starch concentration

Dongling Qiao[a], Wenyao Tu[a], Zhong Wang[a], Long Yu[b,d], Binjia Zhang[c] *, Xianyang Bao[b,d], Fatang Jiang[a,e] *, Qinlu Lin[f]

[a] *Glyn O. Phillips Hydrocolloid Research Centre at HBUT, School of Food and Biological Engineering, Hubei University of Technology, Wuhan, Hubei 430068, China*

[b] *Centre for Polymer from Renewable Resource, South China University of Technology, Guangzhou, Guangdong 510640, China*

[c] *Key Laboratory of Environment Correlative Dietology (Ministry of Education), College of Food Science and Technology, Huazhong Agricultural University, Wuhan, Hubei 430070, China*

[d] *Department of Materials Engineering, Monash University, Melbourne, Vic 3168, Australia*

[e] *Faculty of Engineering, University of Nottingham, Nottingham NG7 2RD, United Kingdom*

[f] *National Engineering Laboratory for Rice and By-product Deep Processing, College of Food Science and Engineering, Central South University of Forestry and Technology, Changsha 410004, China*

* Corresponding authors. *Email addresses*: zhangbj@mail.hzau.edu.cn (B. Zhang); jiangft@mail.hbut.edu.cn (F. Jiang).

Abstract: This work concerns how crosslinker amount (*N, N'*-methylene-bisacrylamide) affects the microstructural, absorbent and rheological features of one-step prepared starch-based superabsorbent polymers at a high starch concentration (0.27:1 w/w starch-water). The increased crosslinker amount evidently altered the microstructure and the absorbent and rheological features. Then, the variations in starch-based superabsorbent polymer properties were discussed from a microstructure viewpoint. Particularly, the higher crosslinker quantity rose the crosslinking density and the ratio (*GR*) of grafted anhydroglucose unit on starch backbone (from 27% to 52%), but short the average polyacrylamide (PAM) chain length (L_{PAM}). These structural features suppressed the chain stretch within starch-based superabsorbent polymer fractal gels (confirmed by smaller R_g value) and promoted the formation of smaller chain networks, thus weakening the water absorption to the starch-based superabsorbent polymer chain networks. Also, the increased *GR* and reduced L_{PAM}, with lowered chain extension and elevated crosslinking density, probably decreased the flexibility and mobility of chain segments in starch-based superabsorbent polymer gel matrixes. This caused the enhanced robustness and storage modulus of the gels with reduced chain energy dissipation ability.

Keywords: starch-based superabsorbent polymer; high-viscosity reaction system; crosslinking agent.

1. Introduction

Superabsorbent polymers (SAPs), as three dimensionally crosslinked hydrophilic polymers, are capable of absorbing and retaining significant amounts of water and the related liquids. With intrinsic advantages over conventional water-absorbing materials such as sponge, cotton and pulp, SAPs have enormous potentials for development of various valuable products such as slow release fertilizers [1, 2], soil conditioners [3], self-healing cementitious materials [4], coal dewatering materials [5], drug delivery systems [6], and hygienic products [7]. Despite these potentials, the SAPs derived from primarily synthetic polymers often show poor biodegradability and renewability, which can cause environmental issues. To address such problems, there has been huge interest in the design of 'greener' SAPs from natural polymers such as starch due to their abundance, biodegradability, renewability, and biocompatibility.

Starch-based SAP (starch-SAP) is a characteristic natural polymer derived SAP, and is normally prepared by solution polymerization. The solution methods involve tedious multi-step reactions (such as polymerization and saponification) and are time-consuming and energy-intensive [8, 9]. Moreover, the starch concentration in common solution systems is relatively low (typically smaller than 10%) [10], due to the high viscosity of gelatinized starch in the reaction system. This low starch content inevitably allows the generation of large quantities of chemical wastes, such as waste water. Therefore, great efforts have been made to develop innovative technologies for cost-effective and eco-friendly preparation of starch-SAPs at high starch concentrations.

In present work, an one-step method, based on a HAAKE twin-roller rotor mixer with oxygen-free reaction atmosphere [11], was established to synthesize starch-SAPs at a high starch concentration (0.27 : 1 w/w starch : water). This one-step mixing method could effectively process the high-viscos reaction materials, and allow the preparation procedures being within just one consecutive step with largely reduced time from 2-3 h to 40 min.

To rationally design starch-SAPs with associated performance, it is indispensable to disclose how the reaction conditions, such as starch features, hydrophilic monomers and crosslinkers, affect the microstructure and application-related properties of starch-SAP. Previous findings have revealed the influence of the reaction conditions such as amylose/amylopectin ratio on the structural features and the properties (*e.g.*, water absorption rate) for starch-SAPs prepared by solution methods and reactive mixing method. The results revealed that the increase in amylose/amylopectin ratio can increase the water absorbent capacity by altering the molecular structure and the network of starch-SAPs on micron scale [10, 12, 13]. Also, the crosslinking density can change the network structure and porosity of SAPs synthesized at low starch concentrations and eventually the absorption behaviors [14]. Nonetheless, it is still unclear how the crosslinking agent amount governs the microstructure and practical properties (*e.g.*, water absorbent capacity and rheological features) of starch-SAP prepared at a high starch concentration using the one-step mixing method mentioned above.

Hence, our work rationalizes the impacts of crosslinking agent on the absorption and rheological behaviors of starch-SAP synthesized at a high starch concentration from a microstructure viewpoint. Particularly, regular maize starch was applied to react with acrylamide monomers, with the presence of a crosslinking agent (*N, N'*-methylene-bisacrylamide (MBA)) and an initiator (ceric ammonium nitrate (CAN)). Then, along with the structure-property results of the starch-SAPs, how the crosslinker influences the absorption and rheological properties of starch-SAP was understood based on the microstructural (molecular and fractal) features. These results are of value for the rational development of starch-SAPs under high material concentrations for various applications with related performance.

2. Materials and Methods

2.1 Materials

Regular maize starch (amylose content 23%) was supplied by Huanglong Food Industry Co., Ltd (China). The original moisture content of maize starch was 13.4%, as measured using a moisture analyzer (MA35, Sartorius Stedim Biotech GmbH, Germany). Other chemicals were of reagent grade, including acrylamide (AM) supplied by Tianjin Kemeou Chemical Reagent Co., Ltd (China), *N,N'*-methylene-bisacrylamide (MBA) acquired from Shanghai Yuanju Biotechnology Co., Ltd (China), and ceric ammonium nitrate (CAN) purchased from Sinopharm Chemical Reagent Co., Ltd (China).

2.2 Starch-SAP synthesis at high starch concentration

A HAAKE Rheocord Polylab RC500p system with a Rhemix 600p twin-roller rotor mixer (ThermoHaake, Germany), was used to prepare starch-SAP samples at a relatively high starch concentration (0.27:1 w/w starch : water), since the mixer could provide high torque to process high-viscous materials. For the samples, 12.0 g of starch (dry basis), 18.0 g of acrylamide, a certain amount of MBA (0.02 g, 0.06 g, 0.10 g, 0.14g or 0.18 g), and 45.0 g of boiling water were placed into the chamber of the HAAKE mixer. Then, at 80 °C chamber temperature, the HAAKE twin-roller rotor mixer kneaded at 80 rpm for 10 min to fully gelatinize the high concentration starch with intense shear stress. Then, N_2 was bubbled into the chamber for 10 min to remove oxygen, and the temperature of the reaction system was cooled to 60 °C. The CAN solution (0.75 g of CAN in 5.0 mL of distilled boiling water) was added, and mixed at 80 rpm for 10 min, followed by addition of sodium hydroxide solution (10.14 g of sodium hydroxide in 10.0 mL of distilled water) for another 10 min mixing. Then, the crude starch-SAP was obtained, and was washed for 5 times with distilled water and 5 times with methanol to remove the free polymer [10]. Each of the fully washed starch-SAPs was dried in an oven at 60 °C to a constant weight, and pulverized through 200 mesh screens.

In the following, codes as “starch-SAP-2” will be used, in which “2” indicates the amount (*i.e.*, 0.02 g) of MBA crosslinking agent used for starch-SAP synthesis.

2.3 Thermogravimetric analysis (TGA)

The proportion (C_{PAM}) of polyacrylamide (PAM) chains grafted in starch-SAP was measured by a PerkinElmer Diamond TGA, according to an earlier report [15]. The starch-SAP was heated from 35 to 600 °C at 10 °C /min in nitrogen atmosphere.

2.4 Nuclear magnetic resonance (NMR) spectroscopy

A Varian NMR 500 system was used to collect the high-resolution ^{13}C NMR spectra at a 125 MHz resonance frequency. The ^{13}C NMR spectra were obtained with a 10 mm solution probe-head at 323.2 K. The chemical shifts of amorphous starch and starch-SAPs were determined using heavy water (D_2O) as internal reference. The grafting of PAM onto starch chain alters the chemical shifts of anhydroglucose carbons and thus generates new peaks nearby original resonances. Thus, relative to the starch, the newly-formed resonances of starch-SAP corresponded to the PAM-grafted starch carbons, and the residual starch resonances of starch-SAP were related to the unreacted starch carbons. Consistently, the ratio (*GR* (%)) of specific starch (anhydroglucose) carbons grafted with PAM and the average length (L_{PAM}) of PAM chains grafted onto starch backbone could be calculated with Eq. (1) and (2).

$$GR = A_{new} / (A_{unreacted} + A_{new}) \times 100\% \quad (1)$$

$$L_{PAM} = (C_{PAM} / M_{AA\text{-}Na}) / (C_{starch} / M_{anhydroglucose} \times GR) \quad (2)$$

In these equations, A_{new} and $A_{unreacted}$ are the resonance peak area for PAM-grafted starch carbons and that for unreacted carbons, respectively; C_{PAM} and C_{starch} are the proportion of PAM and that of starch in starch-SAP, respectively; $M_{AA\text{-}Na}$ and $M_{anhydroglucose}$ are the molar mass of sodium acrylate and that of anhydroglucose, respectively.

2.5 Synchrotron small angle X-ray scattering (SAXS)

The SAXS/WAXS beamline (flux, 1013 photons/s) at the Australian Synchrotron (Clayton, Vic, Australia) was applied to conduct the SAXS experiments at a X-ray wavelength λ = 1.47 Å. The 2D scattering data were recorded by a Pilatus 1M camera (active area 169 × 179 mm; pixel size 172 × 172 μm) and were transformed into the one-dimensional scattering patterns with the scatterbrain software. The swollen starch-SAPs were used as the samples, and the scattering of pure water with a Kapton tape (5413 AMBER 3/4IN X 36YD, 3 M, USA) on the stage window was used as the background data. All of the scattering data were background subtracted and normalized.

The patterns in the angular range of $0.015 < q < 0.20$ Å^{-1} were used as the SAXS data ($q = 4\pi\sin\theta/\lambda$, where 2θ is the scattering angle and λ is the wavelength of the X-ray source). The SAXS patterns were fitted using a unified model (Eq. 3) [16-18].

$$I(q) = G\exp\left(-\frac{R_g^2 q^2}{3}\right) + B\left(\frac{(\mathrm{erf}(qR_g/\sqrt{6}))^3}{q}\right)^p \tag{3}$$

Here, G is the pre-factor of the Guinier function corresponding to a radius R_g; B and p are the pre-factor and the exponent of the power-law function, respectively.

2.6 Water absorbent capacity (WAC)

A home-made bag (300 mesh screen cloth; 4×13 cm) containing *ca*. 0.50 g of dried starch-SAP was immersed into excess distilled water to soak at ambient temperature (26 °C) for 1 h. Then, the free water was removed from the bag using paper towel, and the weight of the swollen starch-SAP was weighed. The *WAC* (g/g) value was calculated based on Eq. (4).

$$WAC = (M_1 - M_2)/M_2 \quad (4)$$

Where M_1 and M_2 (g) is the weight of swollen starch-SAP and that of dried starch-SAP, respectively. All the results were the averages of three replicates.

2.7 Rheological features

The rheological properties of swollen starch-SAPs, absorbing the same amount of water (50 g/g), were evaluated using a controlled stress rheometer (Discovery HR-2, TA, USA) with a cone plate (diameter 40 mm; cone angle 1°) at a gap of 1.0 mm. Oscillatory strain sweeps of swollen starch-SAP samples were performed at 1 rad/s and at 25 °C in a strain range of 0.1~100 %. The frequency sweeps were done at 1 % strain and at 25 °C in a frequency range of 0.01~100 rad/s.

2.8 Statistical analysis

Data were expressed as means ± standard deviations (SD). A statistical difference of $P < 0.05$ was considered to be significant. Linear regression fitting and regression analysis were carried out in Microsoft Excel 2010 (Redmond, WA, USA).

3. Results and discussion

3.1 TGA analysis for C_{PAM}

The thermogravimetric (TG) curve and its derivative (DTG) curve of starch-SAP-2 are presented in **Fig. 1a**, and the TG curves of starch-SAPs are shown in **Fig. 1b**. The DTG curve of starch-SAP-2 revealed three unambiguous stages for the decomposition of starch-SAP. According to earlier findings [15], the three stages were related to the dehydration (*ca*. 30-200 °C), the degradation of starch (*ca*. 250-350 °C) and the PAM chains on starch-SAPs (*ca*. 380-570 °C). There were no apparent differences in the thermal degradation temperature among the starch-SAPs (**Fig. 1b)**. Using the percentage of each weight loss on DTG curves, the PAM contents (C_{PAM}) in starch-SAPs were calculated [19] and are listed in **Table 1**. The five starch-SAPs did not show significant differences in C_{PAM}, indicating that the MBA crosslinker content negligibly affected the amount of PAM chains grafted on the starch-SAPs.

3.2 ^{13}*C NMR analysis for GR* and L_{PAM}

The ^{13}C NMR spectra of starch and starch-SAPs are shown in **Fig. 2**. Consistent with earlier reports [20, 21], the C1 to C6 carbons in starch anhydroglucose units were clearly identified, including the peaks at *ca*. 101.0 and 79.4 ppm for C1 and C4 respectively, the resonance peaks between 74.2 and 72.4 ppm for C2, C3, and C5, and the peak at *ca*. 61.5 ppm for C6. Other than the C1 to C6 resonances on anhydroglucose units, the starch-SAPs exhibited additional resonances in the range of 183.3-77.2 ppm for the amide carbonyl of PAM and the resonances between 49.3 and 36.1 ppm for the hybridized carbon $(CH_2CH)_n$ units of PAM chains [22]. In addition, there were new peaks presenting nearby the C2, C3 and C5 of starch anhydroglucose units, indicating that part of the three carbons were grafted with PAM and thus had alterations in chemical shifts.

Graft polymerization of acrylamide onto starch was initiated by generating free radicals on starch chains, followed by grafting acrylamide onto starch backbone [23]. The ratio (*GR*) of C2, C3 and C5 grafted with PAM and the average length (L_{PAM}) of PAM chains grafted onto starch backbone are recorded in **Table 1**. The increase in MBA amount could increase the value of *GR* but reduce the value of L_{PAM}. As we known, the MBA could graft directly onto C2, C3 and C5 in anhydroglucose units, or onto PAM chains. The latter case would terminate the PAM chain propagation and contribute to the grafting of AMs onto anhydroglucose units. Thus, the higher amount of MBA allowed more C2, C3 and C5 involved into the graft reaction (as reflected by the increment of *GR*). Since L_{PAM} (the average length of PAM chains) was positively correlated to C_{PAM} and negatively related to *GR* (Eq. 2), the negligibly evolved C_{PAM} and the evidently increased *GR* could result in a gradual reduction in the L_{PAM} as the amount of MBA rose.

3.3 Fractal structure of starch-SAP gels

Fig. 3 includes the SAXS patterns of starch-SAPs after water absorption. The swollen starch-SAPs exhibited an inflection point at about 0.04-0.05 $Å^{-1}$, correlated with the Guinier scattering behavior from a structure with a radius of gyration R_g (Å) [18, 24]. In present work, R_g can be ascribed to the size of fractal gels formed by starch chains, PAM chains and water molecules. **Table 1** lists the fitted R_g and the power law exponent (p) for starch-SAPs. The p value can be used to describe the disordered objects which displayed geometrically self-similar structure under transformation of scale. The p value ranged from approximately 1.50 to 1.95, indicating that the starch-SAP gels showed a mass fractal structure (Beaucage, 1996). For the mass fractal structure, the p value (equal to mass fractal dimension D_m) is positively related to the compactness of the structure [25]. In **Table 1**, the mass fractal gels of starch-SAP-2 displayed a R_g value of 96.5 Å and a p value of 1.51. When a higher amount of MBA was used, there were a reduction in R_g and an increase in p

for starch-SAP mass fractal gels. That is, the increase in MBA crosslinker could restrict the chain extensions within the mass fractal gels constructed by starch and PAM chains with water molecules.

3.4 Water absorbent capacity (WAC)

Table 1 also presents the *WAC* results for the starch-SAPs prepared under the high starch concentration. The results revealed that the increased MBA amount resulted in a reduced *WAC*. This reduction could be associated with the variations in the microstructural features of starch-SAPs (illustrated in **Fig. 4**). Previous results revealed that the *WAC* of starch-SAP was associated with the PAM content due to the hydrophilicity difference for functional groups on starch and PAM chains. It is also related to the average chain length of PAM since a larger average chain length could lead to the formation of relatively larger networks for starch-SAP and allow it hold more water molecules [12]. In the present study, the increase of MBA crosslinker allowed the unaffected content of hydrophilic PAM chains in the SAPs (shown by unchanged C_{PAM}), the increased ratio of starch carbons grafted with PAM chains (reflected by increased *GR*), and the shortened average length of PAM chains (revealed by reduced L_{PAM}). Together with the increased crosslinking density, such structural features (the higher *GR* and the smaller L_{PAM}) not only suppressed the chain extensions within the starch-SAP gels, as confirmed by the reduced fractal gel size R_g with increased compactness p, but also were preferable for the formation of starch-SAP chain networks with a reduced size. In this way, the absorbing (and holding) events of water molecules into the molecule chain networks of the starch-SAPs could be weakened, which induced a reduction in the water absorbent ability indicated by *WAC*.

3.5 Rheological properties of starch-SAP gels

Fig. 5 includes the storage modulus (G') profiles under oscillatory strain sweeps and frequency sweeps, and the loss factor (tan δ) profiles under frequency sweeps for the starch-SAPs prepared at the high starch concentration. As presented in **Fig. 5a**, the G' plots possessed a similar linear viscoelastic region (LVR) below 2%-3% strains for the starch-SAPs. Then, a strain of 1% was used to conduct the frequency sweeps to ensure a linear viscoelastic response. In the whole frequency range, the starch-SAPs showed dominantly elastic features ($G' > G''$) (**Fig. 5b** and **Fig. S1** in supplementary material). In **Fig. 5b**, the starch-SAP-2 gel had a more prominent increase in G' as the frequency rose than did other SAPs, indicating less robust gel matrixes. Also, the increased MBA induced an overall increase in G' profile.

In fact, for crosslinked polymer, the chains between the junction points (*viz*., "chains in-between") dominantly response to the external stress via chain compression or stretch [26]. The swollen starch-SAPs contained predominantly two kinds of "chains in-between", including the PAM chains with one end linked to -OH on anhydroglucose units and the other end to MBA crosslinker and the segments of starch chains with two ends grafted by PAM chains (see **Fig. 4a**). The higher MBA amount increased the ratio of starch carbons grafted with PAM (shown by the larger *GR*), and topologically divided the starch chains into shorter fragments. These shortened chain segments and the reduced PAM chain length (indicated by the smaller L_{PAM}) could display greater rigidity than the longer counterparts, and eventually displayed robustness and storage modulus for the starch-SAP gel matrixes. In addition, the increased crosslinking density and the less stretched starch-SAP chains (shown by the reduced size and the increase density for the mass fractal gels) also contributed to enhancing the resistance of the gel matrixes to external stress (the higher robustness and storage modulus) (**Fig. 4b**).

Furthermore, the loss factor tan δ (defined as G''/G') is an indicator of the energy dissipated by the internal friction between the starch-SAP chains upon their movement. **Fig. 5c** includes the loss factor patterns for the starch-SAPs which had a peak at around 40 Hz. This loss factor peak indicated

the energy dissipation maximum throughout the frequency range used. Note that the intensity of tanδ peak gradually reduced with the MBA amount rising. Like the discussion for storage modulus, using more MBA crosslinker led to the increased ratio of starch carbons grafted, the shortened PAM chains, the risen crosslinking density and the weakened stretch of molecule chains. These tended to reduce the flexibility of chains within starch-SAP gel, thus resulting in the lower mobility of the chains (a reduced strain under the same external stress). As a consequence, the mechanical energy dissipation of starch-SAP chains during the testing displayed a decreasing trend with the MBA amount rose (**Fig. 4b**).

4. Conclusions

This work has revealed how the MBA crosslinker amount influences the microstructure and the absorbent and rheological features for starch-SAPs prepared by a one-step method at the high starch concentration. Note that the increase in MBA amount could substantially alter the microstructural features and thus the absorbent and rheological properties of starch-SAPs. Then, the evolutions in starch-SAP properties were discussed from a viewpoint of microstructure.

Specifically, other than the increment of crosslinking density, the higher quantity of MBA allowed the increased ratio (*GR*) of starch carbons grafted by PAM, and the shortened average length (L_{PAM}) of PAM chains. Such structural features certainly suppressed the chain stretch within starch-SAP mass fractal gels, and contributed to the formation of starch-SAP chain networks with a reduced size; this weakened the absorbing (and holding) events of water molecules into the molecule chain networks of starch-SAP matrixes. Then, a reduction in the water absorbent ability occurred with the MBA amount rose. On the other hand, the reduced *GR* and L_{PAM}, with lowered chain extension and elevated crosslinking density, decreased the flexibility and mobility of chain segments within the starch-SAP gel matrixes. Consequently, the starch-SAP gels showed the enhanced robustness and

storage modulus as well as the reduced energy dissipation (reflected by loss factor) of chains. In addition, the results confirmed that the starch-SAPs with higher *WAC* displayed the lower robustness and storage modulus, indicating a lower capability to keep water for those SAPs related to their relatively low crosslinking density.

The present work enables a well understanding of the properties of one-step prepared starch-SAPs at high starch concentration, and thus is valuable for rationally developing 'greener' starch-SAPs for versatile applications with tailored properties.

Acknowledgment

The authors would like to acknowledge the National Natural Science Foundation of China (31801582, 31701637 and 31671827), the Fundamental Research Funds for the Central Universities (2662016QD008), and the European Commission for the H2020 Marie Skłodowska-Curie Actions Individual Fellowships-2017 Project (794680). This research was partially undertaken on the SAXS/WAXS beamline at the Australian Synchrotron, Victoria, Australia. B. Zhang also thank the Young Elite Scientists Sponsorship Program by China Association for Science and Technology.

References

[1] X. Xiao, L. Yu, F. Xie, X. Bao, H. Liu, Z. Ji, L. Chen, One-step method to prepare starch-based superabsorbent polymer for slow release of fertilizer, Chem. Eng. J., 309 (2017) 607-616.

[2] D. Qiao, H. Liu, L. Yu, X. Bao, G.P. Simon, E. Petinakis, L. Chen, Preparation and characterization of slow-release fertilizer encapsulated by starch-based superabsorbent polymer, Carbohydr. Polym., 147 (2016) 146-154.

[3] A.M. Elbarbary, H.A.A. El-Rehim, N.M. El-Sawy, E.-S.A. Hegazy, E.-S.A. Soliman, Radiation induced crosslinking of polyacrylamide incorporated low molecular weights natural polymers for possible use in the agricultural applications, Carbohydr. Polym., 176 (2017) 19-28.

[4] D. Snoeck, K.V. Tittelboom, S. Steuperaert, P. Dubruel, N.D. Belie, Self-healing cementitious materials by the combination of microfibres and superabsorbent polymers, J. Intell. Mater. Syst. Struct., 25 (2014) 13-24.

[5] S. Zhang, H. Chen, S. Liu, J. Guo, Superabsorbent Polymer with High Swelling Ratio, and Temperature-Sensitive and Magnetic Properties Employed as an Efficient Dewatering Medium of Fine Coal, Energy & Fuels, 31 (2017) 1825-1831.

[6] M.T. Haseeb, M.A. Hussain, S.H. Yuk, S. Bashir, M. Nauman, Polysaccharides based superabsorbent hydrogel from Linseed: Dynamic swelling, stimuli responsive on–off switching and drug release, Carbohydr. Polym., 136 (2016) 750-756.

[7] N. Peng, Y. Wang, Q. Ye, L. Liang, Y. An, Q. Li, C. Chang, Biocompatible cellulose-based superabsorbent hydrogels with antimicrobial activity, Carbohydr. Polym., 137 (2016) 59-64.

[8] P. Lanthong, R. Nuisin, S. Kiatkamjornwong, Graft copolymerization, characterization, and degradation of cassava starch-g-acrylamide/itaconic acid superabsorbents, Carbohydr. Polym., 66 (2006) 229-245.

[9] S. Pal, T. Nasim, A. Patra, S. Ghosh, A. Panda, Microwave assisted synthesis of polyacrylamide grafted dextrin (Dxt-g-PAM): Development and application of a novel polymeric flocculant, Int. J. Biol. Macromol., 47 (2010) 623-631.

[10] W. Zou, L. Yu, X. Liu, L. Chen, X. Zhang, D. Qiao, R. Zhang, Effects of amylose/amylopectin ratio on starch-based superabsorbent polymers, Carbohydr. Polym., 87 (2012) 1583-1588.

[11] D. Qiao, W. Zou, X. Liu, L. Yu, L. Chen, H. Liu, N. Zhang, Starch modification using a twin‐roll mixer as a reactor, Starch‐Stärke, 64 (2012) 821-825.

[12] D. Qiao, L. Yu, X. Bao, B. Zhang, F. Jiang, Understanding the microstructure and absorption rate of starch-based superabsorbent polymers prepared under high starch concentration, Carbohydr. Polym., 175 (2017) 141-148.

[13] X. Xiao, L. Yu, F. Xie, X. Bao, H. Liu, Z. Ji, L. Chen, One-step method to prepare starch-based superabsorbent polymer for slow release of fertilizer, Chem. Eng. J., 309 (2017) 607-616.

[14] K. Kabiri, H. Omidian, S.A. Hashemi, M.J. Zohuriaan-Mehr, Synthesis of fast-swelling superabsorbent hydrogels: effect of crosslinker type and concentration on porosity and absorption rate, Eur. Polym. J., 39 (2003) 1341-1348.

[15] W. Zou, X. Liu, L. Yu, D. Qiao, L. Chen, H. Liu, N. Zhang, Synthesis and Characterization of Biodegradable Starch-Polyacrylamide Graft Copolymers Using Starches with Different Microstructures, J. Polym. Environ., 21 (2013) 359-365.

[16] G. Beaucage, Small-angle scattering from polymeric mass fractals of arbitrary mass-fractal dimension, J. Appl. Crystallogr., 29 (1996) 134-146.

[17] J. Doutch, M. Bason, F. Franceschini, K. James, D. Clowes, E.P. Gilbert, Structural changes during starch pasting using simultaneous Rapid Visco Analysis and small-angle neutron scattering, Carbohydr. Polym., 88 (2012) 1061-1071.

[18] B. Zhang, L. Chen, F. Xie, X. Li, R.W. Truss, P.J. Halley, J.L. Shamshina, R.D. Rogers, T. McNally, Understanding the structural disorganization of starch in water-ionic liquid solutions, Phys. Chem. Chem. Phys., 17 (2015) 13860-13871.

[19] D. Qiao, X. Bao, X. Liu, L. Chen, X. Zhang, P. Chen, Preparation of cassava starch-based superabsorbent polymer using a twin-roll mixer as reactor, Chin. J. Polym. Sci., 32 (2014) 1348-1356.

[20] I. Tan, B.M. Flanagan, P.J. Halley, A.K. Whittaker, M.J. Gidley, A Method for Estimating the Nature and Relative Proportions of Amorphous, Single, and Double-Helical Components in Starch Granules by 13C CP/MAS NMR, Biomacromolecules, 8 (2007) 885-891.

[21] B. Zhang, F. Xie, J.L. Shamshina, R.D. Rogers, T. McNally, P.J. Halley, R.W. Truss, L. Chen, S. Zhao, Dissolution of Starch with Aqueous Ionic Liquid under Ambient Conditions, ACS Sustainable Chemistry & Engineering, 5 (2017) 3737-3741.

[22] G. Sen, S. Pal, in: Macromolecular symposia, Wiley Online Library, 2009, pp. 100-111.

[23] B. Raj Sharma, V. Kumar, P.L. Soni, Ceric ammonium nitrate-initiated graft copolymerization of acrylamide onto Cassia tora gum, J. Appl. Polym. Sci., 86 (2002) 3250-3255.

[24] D. Qiao, F. Xie, B. Zhang, W. Zou, S. Zhao, M. Niu, R. Lv, Q. Cheng, F. Jiang, J. Zhu, A further understanding of the multi-scale supramolecular structure and digestion rate of waxy starch, Food Hydrocolloid, 65 (2017) 24-34.

[25] T. Suzuki, A. Chiba, T. Yarno, Interpretation of small angle X-ray scattering from starch on the basis of fractals, Carbohydr. Polym., 34 (1997) 357-363.

[26] M. Rubinstein, S. Panyukov, Elasticity of Polymer Networks, Macromolecules, 35 (2002) 6670-6686.

392 **Figure Captions**

393 **Fig. 1** TG and DTG curves of starch-SAP-2 (a), and TG curves of starch-SAPs (b) (starch-SAP-2,
394 starch-SAP-6, starch-SAP-10, starch-SAP-14, and starch-SAP-18).

395 **Fig. 2** NMR spectra of amorphous starch and starch-SAPs prepared at high starch concentration
396 (starch-SAP-2, starch-SAP-6, starch-SAP-10, starch-SAP-14, and starch-SAP-18) with an inserted
397 schematic structure for anhydroglucose unit.

398 **Fig. 3** SAXS patterns and their fit curves of starch-SAPs prepared at high starch concentration
399 (starch-SAP-2, starch-SAP-6, starch-SAP-10, starch-SAP-14, and starch-SAP-18).

400 **Fig. 4** Schematic representation for formation of three-dimensional network of starch-SAP (a), and
401 for how crosslinker amount affects the water absorbent and rheological features of starch-SAP (b).

402 **Fig. 5** Storage modulus (G') plots under oscillatory strain sweeps (a) and under frequency sweeps
403 (b), and loss factor tan δ plots under frequency sweeps (c) for the starch-SAPs.

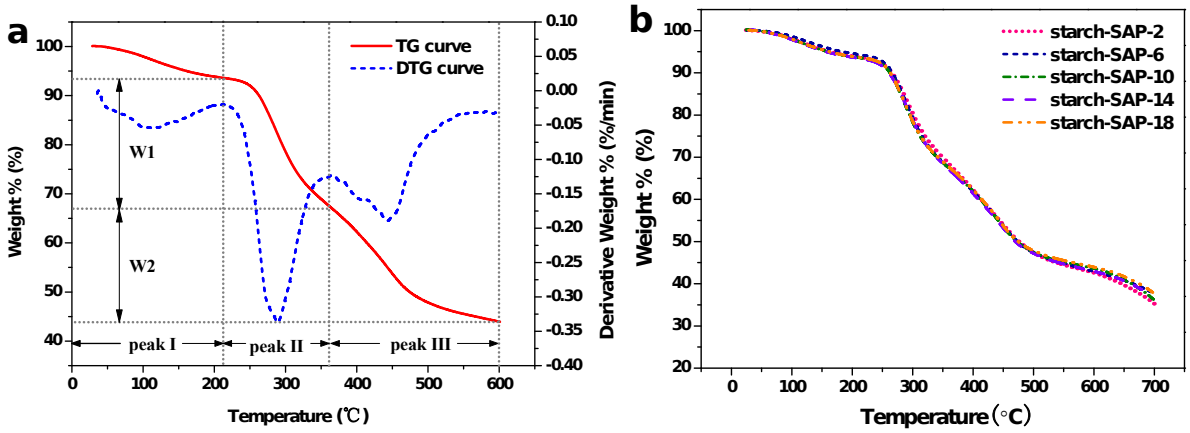
a
TG curve
DTG curve
W1
W2
peak I
peak II
peak III
Weight % (%)
Derivative Weight % (%/min)
Temperature (℃)
b
starch-SAP-2
starch-SAP-6
starch-SAP-10
starch-SAP-14
starch-SAP-18
Weight % (%)
Temperature (°C)

Fig. 1

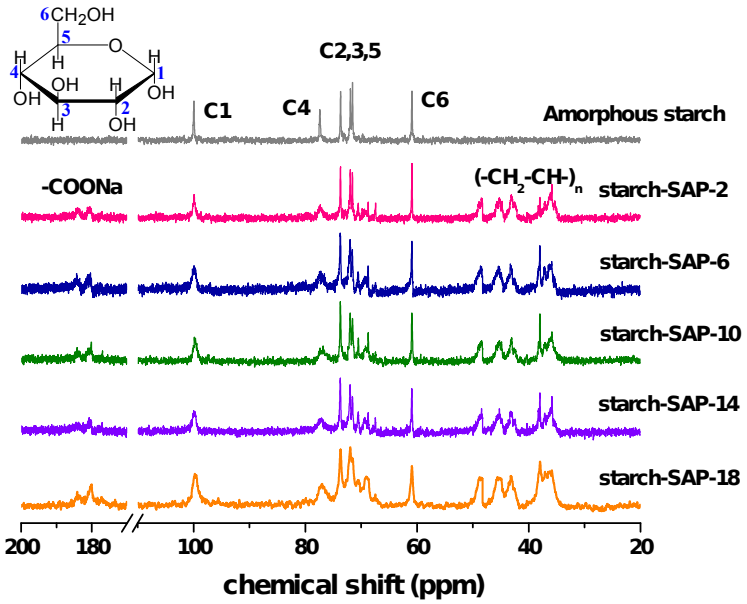
6CH2OH
5
O
H
H
4
1
OH
H
OH
OH
3
2
H
OH
C1
C4
C2,3,5
C6
Amorphous starch
-COONa
(-CH2-CH-)n
starch-SAP-2
starch-SAP-6
starch-SAP-10
starch-SAP-14
starch-SAP-18
200
180
100
80
60
40
20
chemical shift (ppm)

Fig. 2

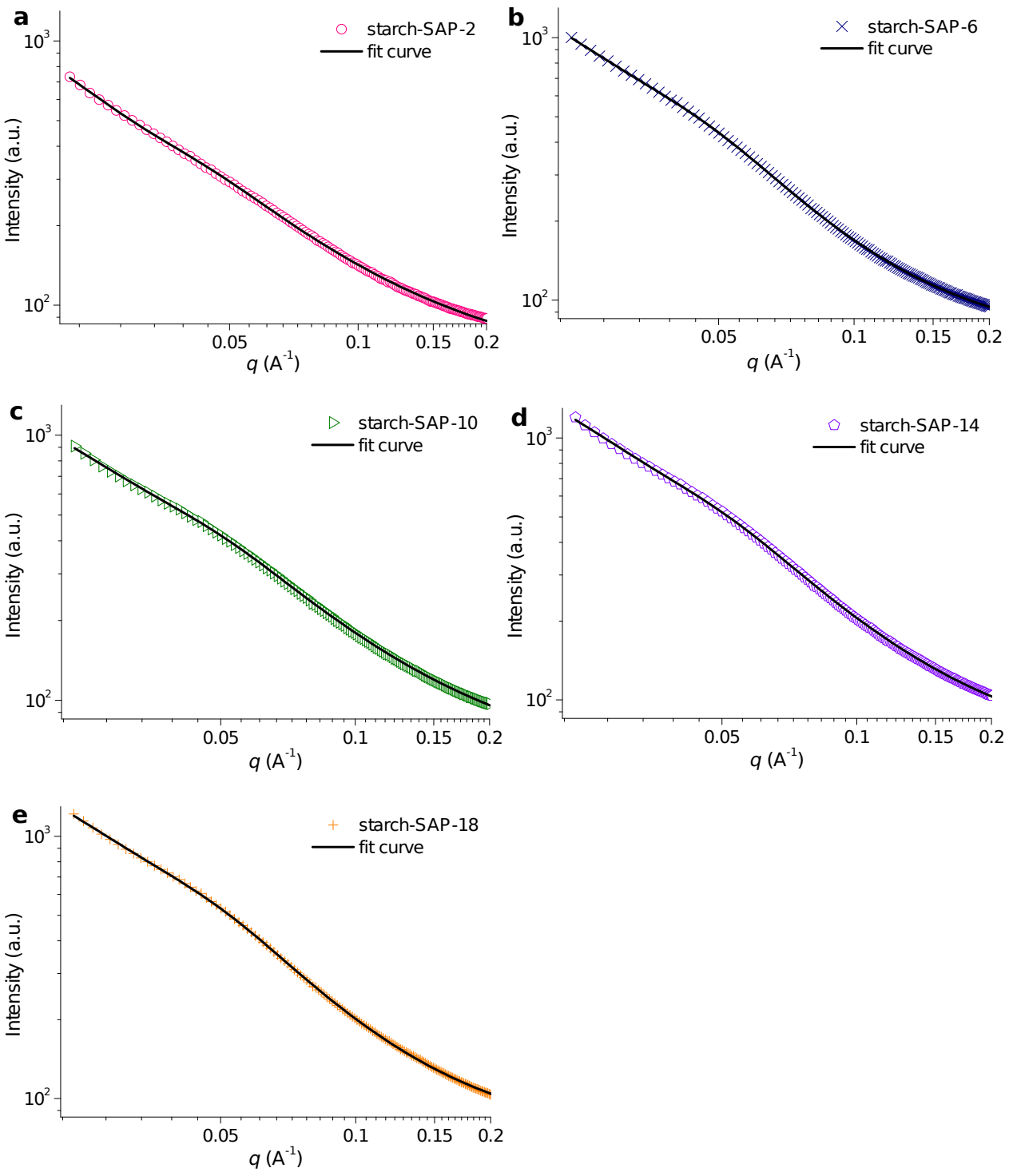
a
starch-SAP-2
fit curve
Intensity (a.u.)
q (A-1)
b
starch-SAP-6
fit curve
c
starch-SAP-10
fit curve
d
starch-SAP-14
fit curve
e
starch-SAP-18
fit curve

Fig. 3

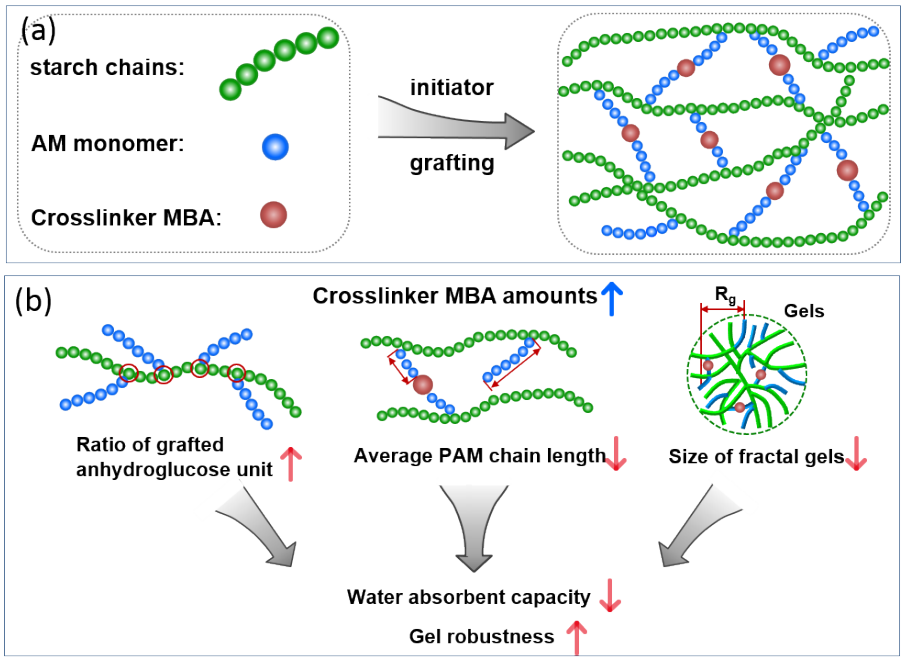
(a)
starch chains:
AM monomer:
Crosslinker MBA:
initiator
grafting
(b)
Crosslinker MBA amounts
Rg
Gels
Ratio of grafted anhydroglucose unit
Average PAM chain length
Size of fractal gels
Water absorbent capacity
Gel robustness

Fig. 4

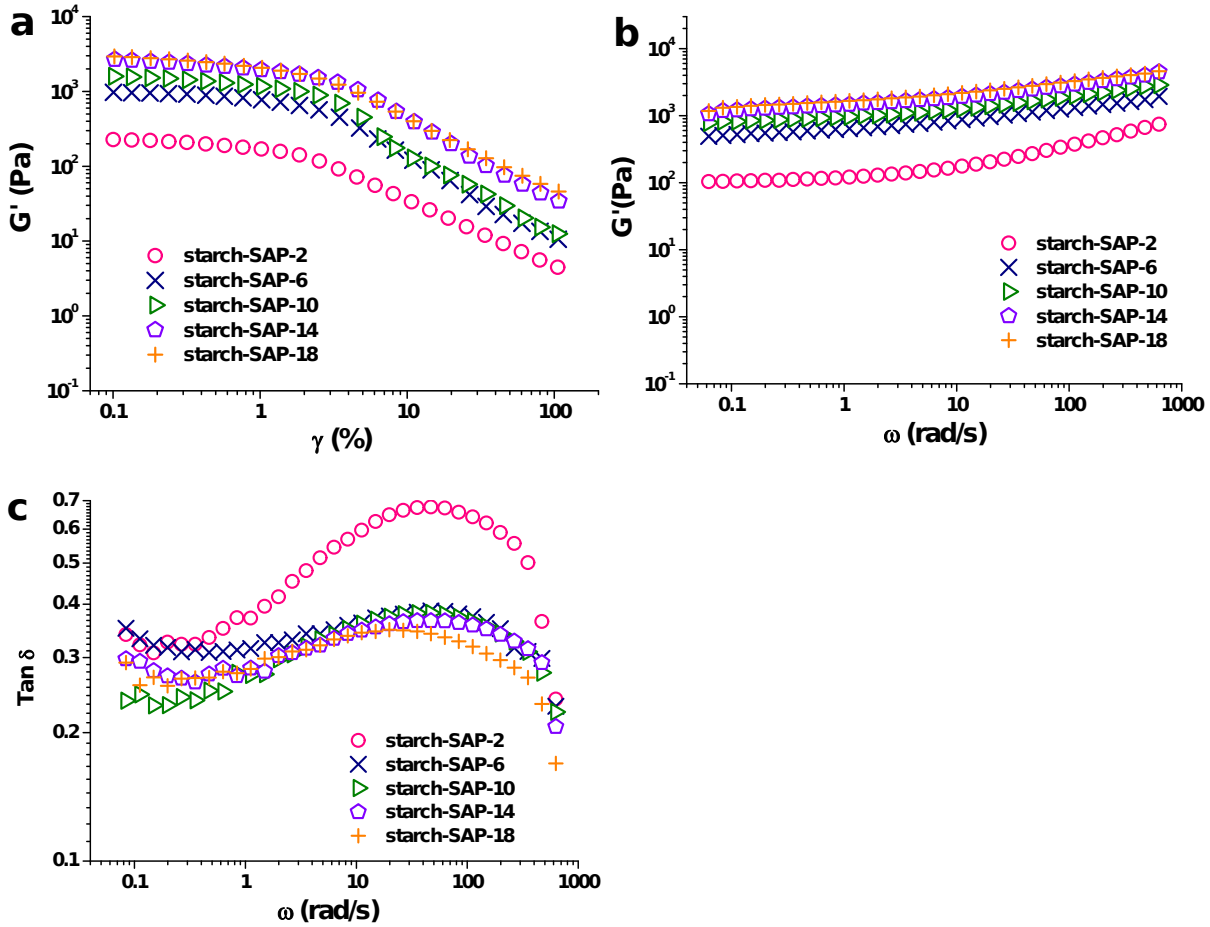
a
G' (Pa)
γ (%)
starch-SAP-2
starch-SAP-6
starch-SAP-10
starch-SAP-14
starch-SAP-18
b
G'(Pa)
ω (rad/s)
starch-SAP-2
starch-SAP-6
starch-SAP-10
starch-SAP-14
starch-SAP-18
c
Tan δ
ω (rad/s)
starch-SAP-2
starch-SAP-6
starch-SAP-10
starch-SAP-14
starch-SAP-18

Fig. 5

417 **Table 1** Molecular parameters of starch-SAPs prepared at high starch concentration (starch-SAP-2,

418 starch-SAP-6, starch-SAP-10, starch-SAP-14, and starch-SAP-18) [A]

	starch-SAP-2	starch-SAP-6	starch-SAP-10	starch-SAP-14	starch-SAP-18
C_{PAM} (%)	50.32±0.23[aB]	49.39±0.83[a]	50.30±1.32[a]	51.20±0.40[a]	49.91±0.26[a]
GR (%)	27.01[d]	25.93[d]	39.39[c]	45.65[b]	52.15[a]
L_{PAM}	6.46[a]	6.49[a]	4.43[b]	3.96[c]	3.29[d]
R_g (Å)	96.5±1.8[a]	83.3±0.5 [b]	82.7±1.4[b]	79.5±1.5[c]	79.9±1.0[c]
p	1.51±0.02[c]	1.97±0.01[a]	1.75±0.03[b]	1.81±0.03[b]	1.95±0.03[a]
WAC (g/g)	212.12±0.51[a]	123.24±1.87[b]	113.85±2.00[c]	110.10±0.50[d]	92.20±1.50[e]

419 [A] Parameter from TGA analysis: C_{PAM}, the proportion of PAM chains grafted on starch-SAP. Parameters from

420 NMR analysis: *GR* (%), the ratio of specific starch (anhydroglucose) carbons grafted with PAM; L_{PAM}, the

421 average length of PAM chains grafted onto starch backbone. Parameters from SAXS analysis: R_g (Å), the

422 radius of fractal gel; *p*, the exponent of the power-law function. Parameter from water absorption testing:

423 *WAC* (g/g), water absorbent capacity.

424 [B] Values followed by the different lowercase letter within a row differ significantly ($P < 0.05$)